arXiv:1609.09612v1 [hep-ph] 30 Sep 2016

ON THE NEW LHC RESONANCE

Paolo Cea [1]

Dipartimento di Fisica, Università di Bari, Bari, Italy

INFN - Sezione di Bari, Bari, Italy

Abstract

We present an alternative interpretation within the Standard Model of the new LHC resonance at 125 GeV. We further elaborate on our previous proposal that the resonance at 125 GeV could be interpreted as a pseudoscalar meson with quantum number $J^{PC} = 0^{-+}$. We develop a phenomenological approach where this pseudoscalar mimics the decays of the Standard Model Higgs boson in the vector boson decay channels. We propose that the true Higgs boson should be a heavy resonance with mass of $750\,GeV$ as argued in Ref. [1]. We determine the most relevant decay modes and estimate the partial decay widths and branching ratios. We also discuss briefly the experimental signatures of this heavy Higgs boson. Finally, we attempt a comparison of our theoretical expectations with recent data at $\sqrt{s} = 13\,TeV$ from ATLAS and CMS experiments in the so-called golden channel. We find that the available experimental data could be consistent with the heavy Higgs scenario.

[1]Electronic address: Paolo.Cea@ba.infn.it

Contents

1 Introduction **3**

2 The Pseudoscalar Resonance at 125 GeV **6**

3 Decay Channels **9**
3.1 $\eta_{tg} \to \gamma\gamma, gg$ 10
3.2 $\eta_{tg} \to Z_0 Z_0, Z_0\gamma$ 12
3.3 $\eta_{tg} \to W^+W^-$ 13
3.4 $\eta_{tg} \to \bar{f}f$ 13
3.5 Partial Widths and Branching Ratios 14

4 Cross Section and Interaction Strengths **14**

5 The H_T Higgs Boson **17**
5.1 H_T Decay Channels 21
5.2 The Golden Channel: Comparison with the LHC Data 22

6 Conclusion **23**

1 Introduction

A cornerstone of the Standard Model is the mechanism of spontaneous symmetry breaking that is now called the Brout-Englert-Higgs (BEH) mechanism [2, 3, 4, 5]. In fact, the discovery of the so-called Higgs boson is one of the primary goals of Large Hadron Collider (LHC) experiments. The first run of proton-proton collisions at the CERN Large Hadron Collider has brought the confirmation of the existence of a boson, named H, which resembles, so far, the one which breaks the electroweak symmetry in the Standard Model of particle physics [6, 7]. The combined ATLAS and CMS experiment best estimate of the mass of the H boson is $m_H = 125.09 \pm 0.24\ GeV$ [8]. Results from both LHC experiments, as summarized in Refs. [9, 10, 11], showed that all measurements of the properties of the new H resonance are consistent with those expected for the Standard Model Higgs boson. Actually, in the LHC Run 1 the strongest signal significance has been obtained from the decays of the H boson into two vector bosons, $H \to VV$ where $V = \gamma, W, Z$. In fact, in these channels the observed signal significance is above $5\ \sigma$ [9, 10, 11]. Moreover, if one introduce the signal strength μ, defined as the ratio of the measured H boson rate to the Standard Model Higgs boson prediction, then it turns out that for these decays $\mu \simeq 1$ within the statistical uncertainties. Nevertheless, these measurements rely predominantly on studies of the boson decay modes. To establish the mass generation mechanism for fermions as implemented in the Standard Model, it is of paramount importance to demonstrate the direct coupling of the H resonance to fermions and the proportionality of its strength to the fermion mass. According to the Standard Model, if one assumes that the H resonance at 125 GeV is the Higgs boson, then the most common decay of H should be a transformation into a pair of $bottom - antibottom$ quarks. Indeed, the $H \to b\,\bar{b}$ decay mode is predicted in the Standard Model to have the largest branching ratio. In spite of this large branching ratio, an inclusive search for $H \to b\,\bar{b}$ is not feasible because of the overwhelming background from multi-jet production. Associated production of a Higgs boson with vector bosons W or Z offers a viable alternative notwithstanding a cross section more than an order of magnitude lower than the inclusive production cross section. In this case a sophisticate statistical analysis is required to fully characterize the background. In general, the number of expected background events and the associated kinematic distributions are derived from a mixture of data-driven methods and simulations. Indeed, the shapes of all backgrounds are estimated from Monte Carlo simulations and maximum likelihood fits. Both the ATLAS and CMS collaborations reported evidences for the $H \to b\,\bar{b}$ mode [12, 13], albeit with a statistical significance of no more than about $3\,\sigma$. It should be mentioned, however, that the ratio of the branching ratios $Br(H \to b\,\bar{b})/Br(H \to Z\,Z)$ displays a deficit of about three standard deviations relatively to the expected Standard Model value [2]. In other words, the H boson seems to decay into a $bottom - antibottom$ pair less frequently than expected. Likewise, the experimental evidence for the $H \to \tau^+\,\tau^-$ decay mode has reached a statistical significance of about $3\,\sigma$ [14, 15]. Finally, the spin and CP properties of the H boson can be determined by studying the tensor structure of its interactions with the electroweak gauge bosons. The experimental analyses [16, 17] rely on discriminant observables chosen to be sensitive to the spin and parity of the signal. Then, a likelihood function that depends on the spin-parity assumption of the signal is constructed. In this way it was possible to compare the Standard Model hypothesis $J^P = 0^+$ to alternative models. The statistic

[2] See Table 9 in Ref. [11].

test used to distinguish between two alternative spin-parity hypotheses was based on the ratio of likelihoods. It turned out that all tested alternative models were excluded with a statistical significance of about $3\,\sigma$ [16, 17]. In particular, the Standard Model hypothesis has been also compared with an alternative spin-zero pseudoscalar boson $J^P = 0^-$. The pseudoscalar hypothesis was implemented with effective higher-dimension operators to describe the interactions of the pseudoscalar boson with the Standard Model vector bosons.

To summarize ATLAS and CMS have combined their analyses for production and decay of the H boson. Up to now, if one identify the H resonance with the Standard Model Higgs boson, then it turns out that many results are in agreements with the Standard Model predictions. However, there are some puzzling deviations with respect to expectations. Aside from the already mentioned deficit in the $bottom - antibottom$ decays, in our opinion the most interesting discrepancy manifest itself in the associate production of the H resonance with a $t\bar{t}$ pair. Indeed, let us introduce the interaction strength $\mu_{t\bar{t}H}$ defined as the ratio of the observed associate production cross section to the expected Standard Model value. The observed value of this interaction strength [11]:

$$\mu_{t\bar{t}H} \;=\; \begin{cases} 2.9\,^{+1.0}_{-0.9} & CMS \quad Run\,1 \\ \\ 1.9\,^{+0.8}_{-0.7} & ATLAS\;\; Run\,1 \end{cases} \tag{1.1}$$

deviates from the Standard Model expectations with a statistical significance of about $2\,\sigma$. Such deviations, if confirmed in the LHC Run 2, may suggest an alternative interpretation of the H resonance. Indeed, in the LHC Run 2 at $\sqrt{s} = 13\,TeV$ the associate production of the Higgs boson with $t\bar{t}$ pairs has a cross section which is about four times larger than in the Run 1. Remarkably, both ATLAS [18] and CMS [19] experiments reported new measurements of the interaction strength $\mu_{t\bar{t}H}$ using LHC collision data at a center of mass energy of $\sqrt{s} = 13\,TeV$ based on an integrated luminosity of $13.3\,fb^{-1}$ and $12.9\,fb^{-1}$ respectively:

$$\mu_{t\bar{t}H} \;=\; \begin{cases} 1.8\,^{+0.7}_{-0.7} & ATLAS\;\; Run\,2 \\ \\ 2.0\,^{+0.7}_{-0.7} & CMS \quad Run\,2 \end{cases} \tag{1.2}$$

Combining the data from Run 1 and Run 2, one obtains:

$$\mu_{t\bar{t}H} \;=\; 2.07 \;\pm\; 0.38 \;\;, \tag{1.3}$$

that would imply a deviation from Standard Model predictions with a statistical significance of about $3\,\sigma$. Obviously, the observed excess could well be a statistical fluctuation. Nevertheless, we believe that by now there are compelling reasons to look for alternative explanations for the new LHC resonance.

Soon after the evidence of the LHC resonance at 125 GeV, we proposed [20] that the H boson could be interpreted as a pseudoscalar meson with quantum number $J^{PC} = 0^{-+}$. The main aim of this paper is to further elaborate the phenomenological approach of Ref. [20]. In particular, in the first part of the paper we will show that our pseudoscalar meson could mimic the decays of the Standard Model Higgs boson in the vector boson decay channels, while the decays into fermions remain strongly suppressed. Now, we recall that the identification of the H resonance with the Standard Model Higgs boson

comes mainly from the decays into two vector bosons that reached a statistical significance above $5\,\sigma$ after the LHC Run 1. Once the pseudoscalar meson could decay into two vector bosons at the same rate as the Higgs boson, to unravel the true nature of the LHC resonance at $125\,GeV$ one must rely heavily on the decay modes into two fermions and the CP assignment of the resonance. In this case, however, the reached statistical significance is well below $5\,\sigma$ and the data display a puzzling deficit in the $b\,\bar{b}$ decay mode. As a consequence the forthcoming LHC Run 2 data will be crucial to the identification of the H resonance at $125\,GeV$ with Standard Model Higgs boson.

Adopting the point of view that the new LHC H resonance is not the Higgs boson of the Standard Model, one faces with the problem of the spontaneous symmetry breaking mechanism and the related scalar Higgs boson. Actually, within the non-perturbative description of spontaneous symmetry breaking in the Standard Model it is known that self-interacting scalar fields are subject to the triviality problem [21]. Usually the spontaneous symmetry breaking in the Standard Model is implemented within the perturbation theory which leads to predict that the Higgs boson mass squared is proportional to $\lambda\,v^2$, where λ is the renormalized scalar self-coupling and $v \simeq 246\ GeV$ is the known weak scale. However, if self-interacting four dimensional scalar field theories are trivial, then $\lambda \to 0$ when the ultraviolet cutoff is send to infinity. Strictly speaking, there are no rigorous proof of triviality. Nevertheless, there exist several numerical studies which leave little doubt on the triviality conjecture. As a consequence, within the perturbative approach, these theories represent just an effective description valid only up to some cut-off scale. On the other hand, in Ref. [1], by means of nonperturbative numerical simulations of the $\lambda\Phi^4$ theory on the lattice, it was enlightened the scenario where the Higgs boson (denoted as H_T in the following [3]) without self-interaction could coexist with spontaneous symmetry breaking. Indeed, due to the peculiar rescaling of the Higgs condensate, the relation between m_{H_T} and the physical v is not the same as in perturbation theory. According to this picture the ratio m_{H_T}/v should be a cutoff-independent constant. Remarkably, extensive numerical simulations showed that the extrapolation to the continuum limit of that ratio leads to a quite sensible result. To appreciate this point, for reader convenience, in Fig. 1 we display the numerical results taken from Fig. 3 of Ref. [1]. From Fig. 1 we see that the continuum limit ($m_{latt} \to 0$) extrapolation of the H_T Higgs boson mass is consistent with the intriguing relation:

$$m_{H_T} \ \simeq \ \pi\ v \tag{1.4}$$

pointing to a rather massive H_T boson, $m_{H_T} \ \simeq \ 750$ GeV. It is worthwhile to stress that the H_T boson mass almost exactly matches the heavy resonance hinted at the early LHC Run 2 in the $\gamma - \gamma$ invariant mass spectrum by both the ATLAS and CMS collaborations [22, 23]. Even though in the new LHC Run 2 data the evidence of the $\gamma - \gamma$ heavy resonance is fading away [24, 25, 26, 27], we shall identify the Standard Model Higgs boson with the $750\,GeV$ resonance H_T. Accordingly, in the second part of the present paper we further elaborate on the production mechanisms of our Higgs boson and try to contrast the theoretical expectations with selected available data collected in the LHC Run 2 experiments.

The remaining of the paper is organized as follows. In Sect. 2 we discuss within the Standard Model our proposal for the pseudoscalar resonance with mass near $125\,GeV$. Sect. 3

[3] The subscript stands for Trivial or, better, True.

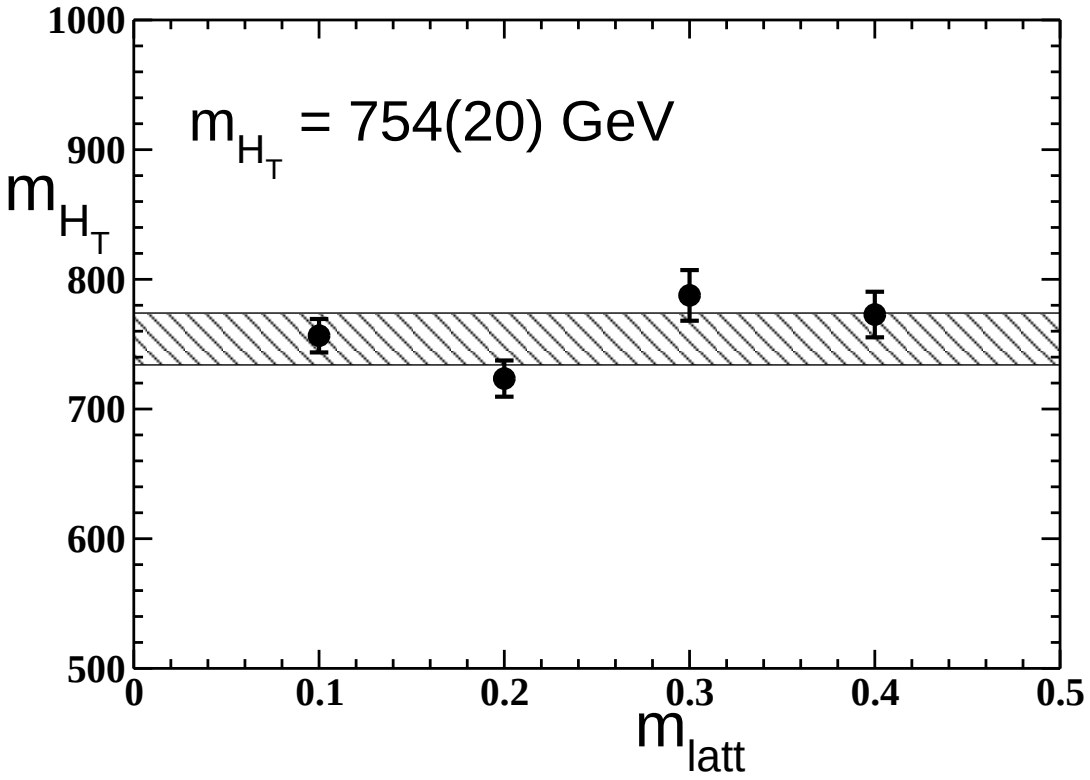

Figure 1: Extrapolation to the continuum limit of the H_T Higgs boson mass. The shaded area corresponds to one standard deviation error in the determination of m_{H_T}. Data adapted from Fig. 3 of Ref. [1].

is devoted to the discussion of the main decay channels of our pseudoscalar meson within a phenomenological approach. In particular, we explicitly evaluate the partial decay widths for the decays in massless vector bosons (Sect. 3.1), in Z_0Z_0 and $Z_0\gamma$ (Sect. 3.2), in W^+W^- (Sect. 3.3), and into fermions (Sect. 3.4). In Sect. 3.5 we estimate the partial decay widths and the resulting branching ratios. In Sect. 4 we discuss the production cross section and estimate the interaction strengths. In Sect. 5 we briefly illustrate the physics of the heavy H_T Higgs boson. We also estimate the expected production cross section. The main decay channels of the H_T Higgs boson are presented in Sect. 5.1, while in Sect. 5.2 we compare our theoretical expectations with the recent data from LHC in the so-called golden channel. Finally, Sect. 6 comprises our concluding remarks.

2 The Pseudoscalar Resonance at 125 GeV

The main aim of the present note is to discuss a possible alternative to the generally assumed Higgs boson interpretation of the new LHC resonance at $125\,GeV$. In our previous paper we looked for alternative explanations within the Standard Model physics. In fact, in Ref. [20] we already suggested that the new resonance could be interpreted as a pseudoscalar meson with quantum number $J^{PC} = 0^{-+}$. The most natural pseudoscalar candidate within the Standard Model is a $q\bar{q}$ bound state with L=S=0. Given the large mass of the new resonance we focused on the pseudoscalar $t\bar{t}$ that, for obviously reasons,

will be referred to as η_t. Since the top quark mass is very large:

$$m_t \simeq 173\, GeV \ , \tag{2.1}$$

to estimate the mass of the pseudoscalar meson η_t, we may safely employ the non-relativistic potential model. Quarkonium potential models typically take the form of a Schrödinger like equation:

$$\left[T + V \right] \Psi = m \Psi \tag{2.2}$$

where T represents the kinetic energy term and V the potential energy term. Equation (2.2) arises from the Bethe-Salpeter equation by replacing the full interaction by an instantaneous local potential. The $quark - antiquark$ potential is typically motivated by the properties expected from QCD. Assuming that at short distances V(r) behaves according to perturbative QCD, then the contribution arising from one-gluon-exchange leads to the Coulomb like potential. At large distances the one-gluon-exchange is no longer a good representation of the $quark - antiquark$ potential. The qualitative picture is that the chromoelectric lines of force bunch together into a flux tube which leads to a distance independent force or linearly rising confining potential. A potential widely used to describe $c\bar{c}$ and $b\bar{b}$ quarkonium states is the so-called Cornell potential [28]:

$$V_C = -\frac{4}{3}\frac{\alpha_c}{r} + \sigma\, r \ , \ \alpha_c \simeq 0.40 \ , \ \sigma \simeq 0.18\, GeV^2 \ . \tag{2.3}$$

The empirical coefficient of the short-distance Coulomb potential $\alpha_c \simeq 0.40$ in the Cornell potential is much larger than the perturbative QCD expectations. This leads to an overestimate of the $q\bar{q}$ bound states for very massive quarks. Alternatively, one may adopt the Richardson potential [29] that incorporates both the QCD asymptotically free short-distance behavior:

$$\lim_{r\to 0} V(r) \sim -\frac{4}{3}\frac{1}{r \ln r} \tag{2.4}$$

and the linear confinement potential at large distances. However, long time ago in Ref. [30] it was showed that if one assumes that $V(r)$ behaves according to Eq. (2.4) for $r \to 0$, then the coupling the $q\bar{q}$ S-wave vector mesons to the electromagnetic current diverges due to the singular behavior of the wavefunction near the origin. This should imply, for instance, that the ratio $R_{e^+e^-}$ is divergent. This divergence is, in fact, an artifact of the instantaneous potential approximation that is not reliable for small enough lengths. Actually, the authors of Ref. [30] found that these spurious divergences could be removed if one assume a constant potential for scales smaller than some high-energy reference scale $\sim 1/M$. In this way one recover the duality between bound states and asymptotically free quarks leading to canonical results for two-point spectral functions of vector and axial-vector currents [30]. Accordingly, we may adopt the Cornell potential Eq. (2.3) where now:

$$\alpha_c \simeq \alpha_s(M) \simeq 0.10 \quad , \quad M \simeq 10^2\, GeV \ , \tag{2.5}$$

with $\alpha_s(M)$ the coupling constant of strong interactions at the scale M. For our purposes it is enough to reach a qualitative estimate of the low-lying $L = S = 0$ bound state. Since the contribution of the linearly rising confining potential can be safely neglected due to the very large top mass, we obtain at once the wave function of the low-lying $L = S = 0$ bound state:

$$\Psi_{00}(r) \simeq \frac{1}{(\pi\, a_0^3)^{\frac{1}{2}}}\, \exp(-\frac{r}{a_0}) \ , \tag{2.6}$$

where a_0 is the Bohr radius:

$$a_0 \;=\; \frac{3}{2\, m_t\, \alpha_c} \;\; . \tag{2.7}$$

We may, then, easily estimate the pseudoscalar mass as follows:

$$m_{\eta_t} \;\simeq\; 2\, m_t \;-\; \frac{4}{3}\, \frac{\alpha_c}{a_0} \;\simeq\; 344\, GeV \; . \tag{2.8}$$

Even though our analysis has been somewhat qualitative, it is evident that the pseudoscalar η_t meson is too heavy to be identified with the new LHC resonance. To overcome this problem we must admit that the η_t meson can have sizable mixing with a much more lighter pseudoscalar meson. In this regard, we observe that the self-coupling of gluons in QCD suggests that additional mesons made of bound gluons (glueballs) may exist. In fact, lattice calculations, flux tube and constituent glue models agree that the lights glueballs have quantum number $J^{PC} = 0^{++}, 2^{++}$ (for a recent review see Refs. [31, 32]). Moreover, there is a general agreements on the existence of pseudoscalar states with $J^{PC} = 0^{-+}$ above $2\, GeV$. In the following we will indicate the lowest glueball pseudoscalar state with η_g and follow the lattice calculations for the mass of the lowest pseudoscalar glueball to set the value [32]:

$$m_{\eta_g} \;\simeq\; 2.6\, GeV \; . \tag{2.9}$$

We see, then, that the pseudoscalar η_t meson can also mix with the pseudoscalar η_g meson through color singlet gluon intermediate states. In this case there are no reasons to restrict the intermediate states to two gluons. In fact, if more gluons are involved then one gets large effective couplings due to the small typical momentum going into each one making the theory strongly coupled [33]. If this is the case, then the large top mass gives rise to a sizable mixing amplitude. We shall proceed as the authors of Ref. [34] did for the mesons η and η'. In fact, if we assume that the annihilation process contribute the flavor independent amount A, we obtain the following mass matrix:

$$\mathcal{M} \;=\; \begin{pmatrix} m_{\eta_g} \,+\, A & A \\ A & m_{\eta_t} \,+\, A \end{pmatrix} \;\; . \tag{2.10}$$

The mass matrix can be easily diagonalized by writing the physical mass eigenstates as:

$$\begin{aligned} \eta_{gt} \;\; &= \;\; \eta_g \, \cos\theta \;\; - \;\; \eta_t \, \sin\theta \\ \eta'_{gt} \;\; &= \;\; \eta_g \, \sin\theta \;\; + \;\; \eta_t \, \cos\theta \end{aligned} \tag{2.11}$$

where θ is the mixing angle. Inverting Eq. (2.11) leads to:

$$\begin{aligned} \eta_g \;\; &= \;\; \eta_{gt} \, \cos\theta \;\; + \;\; \eta'_{gt} \, \sin\theta \\ \eta_t \;\; &= \;\; \eta'_{gt} \, \cos\theta \;\; - \;\; \eta_{gt} \, \sin\theta \;\; . \end{aligned} \tag{2.12}$$

We denote with η_{gt} the state with lowest mass eigenvalue. Moreover we impose that:

$$m_{\eta_{gt}} \;\simeq\; 125\, GeV \; . \tag{2.13}$$

Then, a standard calculation gives:

$$m_{\eta'_{gt}} \simeq 776\, GeV \quad , \quad \theta \simeq 29^\circ \ . \tag{2.14}$$

Since the mass eigenstate η'_{gt} lies well above the $t\bar{t}$ threshold, it hardly can be detected as a hadronic resonance. On the other hand, the eigenstate η_{gt} could be a serious candidate for the new resonance detected at LHC. To corroborate these expectations we need to estimate the total width and the decay channels of the pseudoscalar meson η_{gt}.

3 Decay Channels

In order to determine the decay rates of the pseudoscalar meson η_{gt} we must take care of the fact that it is a mixture of the pseudoscalar glueball η_g and the pseudoscalar $t\bar{t}$ bound state η_t. In general, the decay width depends on the wave function. Since $m_t \gg m_{\eta_g}$, from Eqs. (2.6) and (2.7) we see that the glueball contributions to the decays can be safely neglected. Thus, for the decay amplitude of η_{gt} into a generic final state F we can write:

$$\mathcal{A}\big(\eta_{gt} \to F\big) \simeq \mathcal{A}\big(\eta_t \to F\big) \, \sin\theta \ . \tag{3.1}$$

To estimate the contribution of the η_t component to the decay width we may use the well known heavy quarkonium model [35, 36] where the decay amplitudes depend on the bound-state wave function at the origin.
Obviously, the most important decay mode is the single-quark decay, leaving the other quark as a spectator. In fact, since the t quark is very heavy this single quark decay becomes the dominant mode of t-quarkonium states, hiding all the other modes. However, observing that the mass of our pseudoscalar $m_{\eta_{tg}} \simeq 125\, GeV$ is smaller than the t quark mass this decay is forbidden. Thus we are left with the decays into two-body final states. Naively, we expect that the main decay channels are given by the decay of η_t into ordinary hadrons that, however, are suppressed by the OZI rule. Therefore, it should turn out that the pseudoscalar meson η_{tg} is rather narrow. Indeed, the pseudoscalar meson decays involve $t\bar{t}$ quarks annihilation. Due to the very high top quark mass the annihilation of a $t\bar{t}$ pair is a short distance process that can be, generally, described by a small effective coupling constant. Therefore one can safely use perturbation theory to find the corresponding transition amplitude. To evaluate the decay rates of the pseudoscalar meson η_{tg} into two-body final states within the Standard Model [4] we shall follow the method developed in Refs. [38, 39, 40]. According to these authors the amplitude for the decay of a given $quark - antiquark$ bound state into any final state is written as the convolution of the scattering matrix element with the relevant wavefunction. We are interested in the case of $L = S = 0$ $quark - antiquark$ bound state with wave function $\Psi_{00}(r)$. Let P^μ be the four-momentum of the bound state, then the decay amplitude can be written as [41]:

$$\mathcal{A}\big(\eta \to F\big) \simeq \frac{1}{2}\sqrt{\frac{3}{M_\eta}}\, \Psi_{00}(0)\, Tr\Big\{\mathcal{O}_F\, \gamma_5\, (-\not{P} + M_\eta)\Big\} \ , \tag{3.2}$$

where the factor $\sqrt{3}$ is due to color. $\mathcal{O}_F$ is obtained from the Feynman-diagram amplitude for a $quark$ with momentum $\frac{P^\mu}{2} + q^\mu$ and an $antiquark$ with momentum $\frac{P^\mu}{2} - q^\mu$ to scatter

[4] In the following we use the convention of Ref. [37].

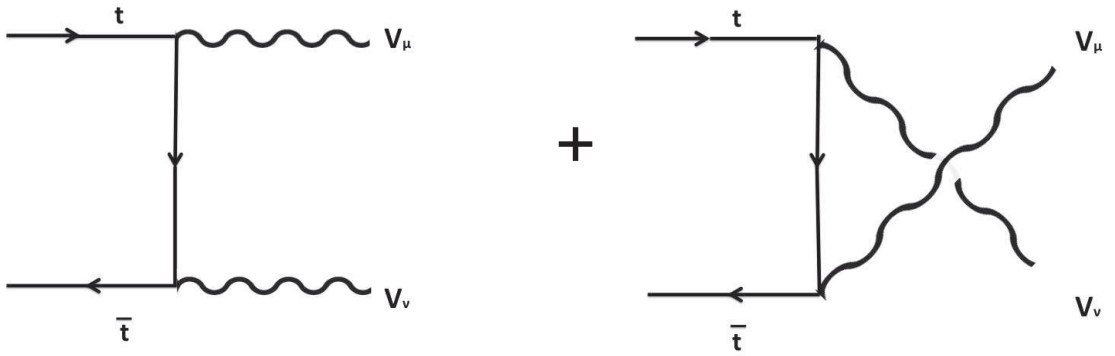

Figure 2: Feynman diagrams contributing to the decay of the pseudoscalar $t\bar{t}$ meson into two vector bosons $V_\mu\, V_\nu$ ($VV = \gamma\gamma, gg, Z_0Z_0, Z_0\gamma$).

into the final state F by removing the spinor factors. For comparison with the literature, we recall that the wavefunction $\Psi_{00}(r)$ is related to the radial wavefunction by:

$$\Psi_{00}(r) \;=\; \frac{1}{\sqrt{4\pi}}\, R_0(r) \;\; . \tag{3.3}$$

3.1 $\eta_{tg} \to \gamma\gamma, gg$

Our aim is to estimate the decay widths of the pseudoscalar meson to two-body final states within the Standard Model. Let us consider, firstly, the decay into two photons. Actually, the widths for the decays to two massless vector states are well known in literature [35, 36]. Indeed, the relevant Feynman diagram are shown in Fig. 2. A standard calculation gives:

$$Tr\Big\{\mathcal{O}_{\gamma\gamma}\,\gamma_5\,(-\not{P} + M_\eta)\Big\} \;\simeq\; 16\pi\alpha\, Q_t^2 \Big\{\frac{1}{2(\frac{P}{2}\cdot k_1)}\,\epsilon_{\mu\nu\rho\sigma}\,\varepsilon_1^\mu\,\varepsilon_2^\nu\,k_1^\rho\,P^\sigma \;+\; (1\to 2)\Big\}\,, \tag{3.4}$$

where $\varepsilon_1^\mu = \varepsilon^\mu(k_1,\lambda_1)$, $\varepsilon_2^\nu = \varepsilon^\nu(k_2,\lambda_2)$, and $Q_t = \frac{2}{3}$ is the top quark electric charge. Therefore, according to our previous discussion, we have:

$$\mathcal{A}\big(\eta_{gt}\to\gamma\gamma\big) \;\simeq\; 8\pi\alpha\, Q_t^2\,\sqrt{\frac{3}{M_{\eta_{gt}}}}\;\Psi_{00}(0)\,\sin\theta\,\Big\{\frac{1}{2(\frac{P}{2}\cdot k_1)}\,\epsilon_{\mu\nu\rho\sigma}\,\varepsilon_1^\mu\,\varepsilon_2^\nu\,k_1^\rho\,P^\sigma \;+\; (1\to 2)\Big\}\,. \tag{3.5}$$

Aside from the $t\bar{t}$ annihilation contribution we need to take care of transition amplitude due to quantum anomalies. Indeed, it is known since long time that the trace and chiral anomalies [42, 43] imply an effective coupling of pseudoscalar mesons to gauge vector fields. For the electromagnetic field this anomalous coupling can be obtained from an effective Lagrangian that, following Ref. [44] is written as:

$$\mathcal{L}_{\gamma\gamma}^{eff}(x) \;\simeq\; \frac{a_{\gamma\gamma}}{\sqrt{6\pi}}\,\frac{\alpha}{f_{\eta_{gt}}}\,F_{\mu\nu}(x)\,\widetilde{F}^{\mu\nu}(x)\,\phi_{\eta_{gt}}(x) \tag{3.6}$$

where $f_{\eta_{gt}}$ is the analogous of the pion decay constant f_π [45]. In Eq. (3.6) $F_{\mu\nu}$ is the electromagnetic field strength tensor, $\widetilde{F}_{\mu\nu} = \frac{1}{2}\epsilon_{\mu\nu\rho\sigma}F^{\rho\sigma}$, and $\phi_{\eta_{gt}}$ is a (pseudo-)scalar interpolating quantum field. For low-mass pseudoscalar mesons, PCAC and low-energy

theorems allow to determine the parameter $a_{\gamma\gamma}$. However, in the present case since both the pseudoscalar glueball η_g and the $t\bar{t}$ pseudoscalar are involved we are not in the position to offer a reliable estimate of $a_{\gamma\gamma}$. Therefore, within our phenomenological approach we leave that parameter as free. Actually, the unknown parameter is the ratio $a_{\gamma\gamma}/f_{\eta_{gt}}$. In the following, for definiteness we assume:

$$f_{\eta_{gt}} \simeq 1.0\, GeV \tag{3.7}$$

while $a_{\gamma\gamma}$ will be a dimensionless parameter. The effective Lagrangian Eq. (3.6) gives rise to an additional transition amplitude:

$$\widetilde{\mathcal{A}}\big(\eta_{gt} \to \gamma\gamma\big) \simeq -\frac{a_{\gamma\gamma}}{\sqrt{6\pi}} \frac{\alpha}{f_{\eta_{gt}}} \frac{1}{2}\, \epsilon_{\mu\nu\rho\sigma} \big[k_1^\mu \varepsilon_1^\nu - k_1^\nu \varepsilon_1^\mu\big]\, \big[k_2^\rho \varepsilon_2^\sigma - k_2^\sigma \varepsilon_2^\rho\big]\, . \tag{3.8}$$

Whereupon, the partial decay width is:

$$\Gamma\big(\eta_{gt} \to \gamma\gamma\big) = \frac{1}{2!}\, \frac{1}{16\pi}\, \frac{1}{m_{\eta_{gt}}} \overline{\Big|\mathcal{A}\big(\eta_{gt} \to \gamma\gamma\big) + \widetilde{\mathcal{A}}\big(\eta_{gt} \to \gamma\gamma\big)\Big|^2}\, , \tag{3.9}$$

where:

$$\overline{\Big|\mathcal{A}\big(\eta_{gt} \to \gamma\gamma\big) + \widetilde{\mathcal{A}}\big(\eta_{gt} \to \gamma\gamma\big)\Big|^2} = \sum_{\lambda_1,\lambda_2} \Big|\mathcal{A}\big(\eta_{gt} \to \gamma\gamma\big) + \widetilde{\mathcal{A}}\big(\eta_{gt} \to \gamma\gamma\big)\Big|^2\, . \tag{3.10}$$

To evaluate the polarization average, we put the top quark on the mass shell and neglect the binding energy so that $m_{\eta_t} \simeq 2m_t$. This ensures the absence of spurious kinematical threshold singularities. After that, to extrapolate to $m_{\eta_{gt}}$ we assumed a dipolar form factor. After some algebra we find:

$$\begin{aligned}\Gamma\big(\eta_{gt} \to \gamma\gamma\big) \simeq \frac{\alpha^2}{32\pi}\, m_{\eta_{gt}} \Bigg\{ & 1536\, \pi^2\, Q_t^4\, \frac{|\Psi_{00}(0)|^2}{m_{\eta_{gt}}^3}\, \sin^2\theta \\ & - \frac{64\pi}{\sqrt{2\pi}}\, Q_t^2\, \frac{a_{\gamma\gamma}}{f_{\eta_{gt}}}\, \frac{\Psi_{00}(0)}{\sqrt{m_{\eta_{gt}}}}\, \sin\theta + \frac{a_{\gamma\gamma}^2}{3\pi}\, \frac{m_{\eta_{gt}}^2}{f_{\eta_{gt}}^2} \Bigg\}\, .\end{aligned} \tag{3.11}$$

Similarly we may calculate the width for the decay into two gluons. As concern the annihilation term, taking into account that the two gluons must be in a color singlet state, the transition rate for $\eta_{gt} \to gg$ can be obtained from the rate in two photons with the replacement $\alpha^2 Q_t^4 \to \frac{2}{9}\alpha_s^2$ [35, 36]. Even in the present case we have an anomalous coupling to the gluon fields that can be accounted for by the effective Lagrangian [44]:

$$\mathcal{L}_{gg}^{eff}(x) \simeq \frac{a_{gg}}{\sqrt{6\pi}}\, \frac{\alpha_s}{f_{\eta_{gt}}}\, G_{\mu\nu}^a(x)\, \widetilde{G}_a^{\mu\nu}(x)\, \phi_{\eta_{gt}}(x) \tag{3.12}$$

The decay width can be obtained by means of calculations very similar to the previous ones. So that, here, we merely present the final result:

$$\begin{aligned}\Gamma\big(\eta_{gt} \to gg\big) \simeq \frac{\alpha_s^2}{32\pi}\, m_{\eta_{gt}} \Bigg\{ & 1024\, \pi^2\, \frac{|\Psi_{00}(0)|^2}{m_{\eta_{gt}}^3}\, \sin^2\theta \\ & - \frac{64\sqrt{\pi}}{3}\, \frac{a_{gg}}{f_{\eta_{gt}}}\, \frac{\Psi_{00}(0)}{\sqrt{m_{\eta_{gt}}}}\, \sin\theta + \frac{a_{gg}^2}{3\pi}\, \frac{m_{\eta_{gt}}^2}{f_{\eta_{gt}}^2} \Bigg\}\, .\end{aligned} \tag{3.13}$$

3.2 $\eta_{tg} \to Z_0 Z_0, Z_0\gamma$

Let us, now, focus on the decays into massive gauge vector bosons. In the present Section we consider the decays into Z_0Z_0 and $Z_0\gamma$, while the decay into two W vector bosons will be discussed in the next Subsection.
The annihilation contribution to the decay $\eta_{gt} \to Z_0Z_0$ can be obtained from the Feynman diagrams in Fig. 2. The corresponding transition amplitude is given by:

$$\mathcal{A}\big(\eta_{gt} \to Z_0 Z_0\big) \simeq \frac{\pi}{2}\,\alpha\,\frac{1+(1-\frac{8}{3}\sin^2\theta_W)^2}{\sin^2\theta_W\cos^2\theta_W}\,\sqrt{\frac{3}{M_{\eta_{gt}}}}\,\Psi_{00}(0)\,\sin\theta\,\times \left\{\frac{1}{(\frac{P}{2}-k_1)^2-m_t^2}\,\epsilon_{\mu\nu\rho\sigma}\,\varepsilon_2^\mu\,\varepsilon_1^\nu\,P^\rho k_1^\sigma \;+\; (1\to 2)\right\}. \tag{3.14}$$

In the same manner we find the following annihilation amplitude for the decay into $Z_0\gamma$:

$$\mathcal{A}\big(\eta_{gt} \to Z_0 \gamma\big) \simeq 2\pi\,\alpha\,Q_t\,\frac{1-\frac{8}{3}\sin^2\theta_W}{\sin\theta_W\cos\theta_W}\,\sqrt{\frac{3}{M_{\eta_{gt}}}}\,\Psi_{00}(0)\,\sin\theta\,\times \left\{\frac{1}{(\frac{P}{2}-k_2)^2-m_t^2}\,\epsilon_{\mu\nu\rho\sigma}\,\varepsilon_2^\mu\,\varepsilon_1^\nu\,k_1^\rho\,P^\sigma \;+\; (1\to 2)\right\}. \tag{3.15}$$

The quantum anomalies are present also for the W and Z couplings. Here, however, the situation is more involved since, in general, the anomalies affect differently the axial and vector coupling to the massive boson vectors. One could take care of this by introducing two more anomalous terms with strengths a_{ZZ} and a_{WW}:

$$\mathcal{L}^{eff}_{ZZ}(x) \simeq \frac{a_{ZZ}}{\sqrt{6\pi}f_{\eta_{gt}}}\,\frac{\alpha}{\sin^2\theta_W\cos^2\theta_W}\,Z_{\mu\nu}(x)\,\widetilde{Z}^{\mu\nu}(x)\,\phi_{\eta_{gt}}(x)\,, \tag{3.16}$$

$$\mathcal{L}^{eff}_{WW}(x) \simeq \frac{a_{WW}}{\sqrt{6\pi}f_{\eta_{gt}}}\,\frac{\alpha}{\sin^2\theta_W}\,W^+_{\mu\nu}(x)\,\widetilde{W}^{-\,\mu\nu}(x)\,\phi_{\eta_{gt}}(x) \;+\; h.c.\,. \tag{3.17}$$

After some standard calculations we find the following decay widths:

$$\Gamma\big(\eta_{gt} \to Z_0 Z_0\big) \simeq \frac{1}{16\pi}\,\frac{\alpha^2}{\sin^4\theta_W\cos^4\theta_W}\,m_{\eta_{gt}}\,\times \left\{24\,\pi^2\left[\frac{1+(1-\frac{8}{3}\sin^2\theta_W)^2}{1-\frac{M_Z^2}{m_t^2}}\right]^2\frac{|\Psi_{00}(0)|^2}{m^3_{\eta_{gt}}}\,\sin^2\theta + \frac{8\pi}{\sqrt{2\pi}}\left[1+(1-\frac{8}{3}\sin^2\theta_W)^2\right]\frac{1-\frac{M_Z^4}{4m_t^4}}{1-\frac{M_Z^2}{m_t^2}}\,\frac{a_{ZZ}}{f_{\eta_{gt}}}\,\frac{\Psi_{00}(0)}{\sqrt{m_{\eta_{gt}}}}\,\sin\theta + \frac{a^2_{ZZ}}{3\pi}\left[1-\frac{M_Z^4}{4m_t^4}\right]\frac{m^2_{\eta_{gt}}}{f^2_{\eta_{gt}}}\right\}, \tag{3.18}$$

and

$$\Gamma\big(\eta_{gt} \to Z_0 \gamma\big) \simeq 6\pi\,\alpha^2\,Q_t^2\,\frac{\left[1+(1-\frac{8}{3}\sin^2\theta_W)^2\right]^2}{\sin^2\theta_W\cos^2\theta_W}\,m_{\eta_{gt}}\left[1+\frac{M_Z^2}{4m_t^2}\right]\frac{|\Psi_{00}(0)|^2}{m^3_{\eta_{gt}}}\,\sin^2\theta\,. \tag{3.19}$$

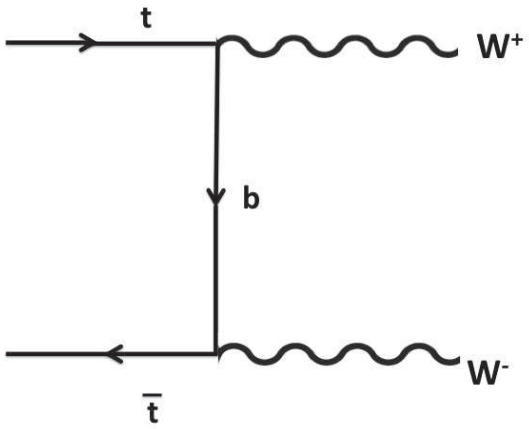

Figure 3: Feynman diagram contributing to the decay of the pseudoscalar $t\bar{t}$ meson into $W^+\,W^-$.

3.3 $\eta_{tg} \to W^+W^-$

Finally, we consider the decay into two vector bosons W^+W^-. The W^+W^- decays are similar to the ZZ decays. There are, however, some differences. In fact, the pseudoscalar meson η_{gt} is allowed to decay into W^+W^- pair by means of the quark-exchange Feynman diagram depicted in Fig. 3, due to the fact that the γ- and Z-exchange diagrams do not contribute [41]. The transition amplitude corresponding to the Feynman diagram in Fig. 3 is readily evaluated:

$$\mathcal{A}\big(\eta_{gt} \to W^+W^-\big) \;\simeq\; \frac{2\pi\alpha}{\sin^2\theta_W}\,|U_{tb}|^2\,\sqrt{\frac{3}{M_{\eta_{gt}}}}\;\frac{\Psi_{00}(0)\,\sin\theta}{(\frac{P}{2}-k_1)^2-m_b^2}\;\epsilon_{\mu\nu\rho\sigma}\;\varepsilon_1^\mu\,\varepsilon_2^\nu\,P^\rho\,k_1^\sigma\;. \quad (3.20)$$

In Eq. (3.20) we considered only the contribution due to the bottom quarks. Since $m_b \ll m_t$, in the following we set $m_b \simeq 0$. Moreover, to a good approximation we may assume for the weak charged-current mixing matrix element $U_{tb} \simeq 1.0$. To obtain the partial decay width we need to consider also the anomalous transition amplitude due to the effective Lagrangian Eq. (3.17). Proceeding as in the previous calculations one finds:

$$\Gamma\big(\eta_{gt} \to W^+W^-\big) \;\simeq\; \frac{1}{16\pi}\,\frac{\alpha^2}{\sin^4\theta_W}\,m_{\eta_{gt}}\,\Bigg\{96\,\pi^2\,\frac{1}{\left[1-\frac{M_W^2}{m_t^2}\right]^2}\,\frac{|\Psi_{00}(0)|^2}{m_{\eta_{gt}}^3}\,\sin^2\theta \quad (3.21)$$

$$+\,\frac{16\pi}{\sqrt{2\pi}}\,\frac{1-\frac{M_W^4}{4m_t^4}}{1-\frac{M_W^2}{m_t^2}}\,\frac{a_{WW}}{f_{\eta_{gt}}}\,\frac{\Psi_{00}(0)}{\sqrt{m_{\eta_{gt}}}}\,\sin\theta\;+\;\frac{a_{WW}^2}{3\pi}\,\left[1-\frac{M_W^4}{4m_t^4}\right]\,\frac{m_{\eta_{gt}}^2}{f_{\eta_{gt}}^2}\Bigg\}\;.$$

3.4 $\eta_{tg} \to \bar{f}f$

The pseudoscalar meson η_{gt} can decay into a fermion-antifermion pairs via the exchange of virtual γ or Z. However, by charge conjugation the γ-exchange contribution vanishes, while the Z-exchange term contributes only through the axial-vector coupling. As a

consequence the transition amplitude turns out to depend on the fermion mass. Therefore, the dominant modes are the $b\bar{b}$ and $\tau^+\tau^-$ decays. The relevant calculations has been already presented in the literature (see, for instance Ref. [41] and references therein). For completeness, we report here the partial decay widths:

$$\Gamma\big(\eta_{gt} \to b\bar{b}\big) \;\simeq\; \frac{9\pi}{8}\,\frac{\alpha^2}{\sin^4\theta_W\cos^4\theta_W}\,|\Psi_{00}(0)|^2\;\sin^2\theta\,\frac{m_b^2}{M_Z^4}\;, \tag{3.22}$$

$$\Gamma\big(\eta_{gt} \to \tau^+\tau^-\big) \;\simeq\; \frac{3\pi}{8}\,\frac{\alpha^2}{\sin^4\theta_W\cos^4\theta_W}\,|\Psi_{00}(0)|^2\;\sin^2\theta\,\frac{m_\tau^2}{M_Z^4}\;. \tag{3.23}$$

3.5 Partial Widths and Branching Ratios

In the previous Sections we have seen that the pseudoscalar meson may mimic the decays expected for the Standard Model Higgs boson. As concern the coupling of the pseudoscalar meson η_{gt} to the gauge vector bosons, it turns out that we can tune the parameters of our model to match as much as possible the branching ratios of the Higgs boson at $125\,GeV$ in the decays into two vector gauge bosons. To estimate the partial decay widths we use the following numerical values:

$$\alpha_s(m_{\eta_{gt}}) \;\simeq\; 0.10\;\;,\;\;\alpha(m_{\eta_{gt}}) \;\simeq\; \frac{1}{127}\;\;,\;\;\sin^2\theta_W \;\simeq\; 0.23\;\;,\;\;\sin^2\theta \;\simeq\; 0.237\,. \tag{3.24}$$

It turns out that the main decay mode of the pseudoscalar η_{gt} is the hadronic decay into two gluons. From Eq. (3.13) one can easily check that the hadronic decay width is comparable to the total decay width of the Standard Model Higgs boson with the same mass. For concreteness, we may tune the parameter a_{gg} such that the total width of the pseudoscalar meson η_{gt} is:

$$\Gamma_{\eta_{gt}} \;\simeq\; 1.0\;MeV\;. \tag{3.25}$$

As concern the other parameter of our phenomenological model, we try to fix the values such as to follow as close as possible the branching ratios of the Standard Model Higgs boson. We found that there are several possibilities. For illustrative purposes we chosen:

$$a_{gg} \;\simeq\; 0.0170\;\;,\;\;a_{\gamma\gamma} \;\simeq\; 0.0145\;\;,\;\;a_{WW} \;\simeq\; -0.00055\;\;,\;\;a_{ZZ} \;\simeq\; -0.0028\,. \tag{3.26}$$

In Table 1 we display the resulting partial decay widths and branching ratios of the η_{gt} pseudoscalar resonance. For comparison we, also, show the branching ratios of the Standard Model Higgs boson. From Table 1 we see, then, that our peculiar pseudoscalar could mimic the decays of the Standard Model Higgs boson in all channels with the exception of the decay into two fermions that turns out to be naturally suppressed. Note that the main decay modes of the pseudoscalar meson are the hadronic decays. However, due to the huge QCD background these decays are extremely difficult to detect experimentally at LHC.

4 Cross Section and Interaction Strengths

In order to check that the new LHC resonance is, indeed, the Standard Model Higgs boson one may compare to observations the rate for production of the Standard Model Higgs

Decay Channel	$\Gamma(\eta_{gt})$	$Br(\eta_{gt})$	$Br(H)$
ZZ	0.0287 MeV	0.0287	0.0266
WW	0.228 MeV	0.228	0.216
$\gamma\gamma$	2.198 KeV	0.0022	0.0023
$Z\gamma$	3.471 KeV	0.0035	0.0016
bb	$3.081\ 10^{-4}$ MeV	$3.081\ 10^{-4}$	0.577
$\tau^+\tau^-$	$1.302\ 10^{-5}$ MeV	$1.302\ 10^{-5}$	0.064
gg	0.747 MeV	0.747	0.086

Table 1: Summary of partial decay widths and branching ratios of the pseudoscalar meson η_{gt}. For comparison we display the Standard Model Higgs boson branching ratios [46].

boson in a given decay channel. To this end, one introduces the relative signal strength defined as the ratio between the observed signal rate from fit to data to the expected Standard Model signal rate at the given mass. The ATLAS and CMS experiments have presented the values of the signal strengths obtained in the LHC Run 1 operations for various decay channels of the H resonance. In particular, in Ref. [11] it is reported the observed values of the H resonance interaction strengths defined by:

$$\mu_F \ = \ \frac{\sigma_H^{obs}\ Br^{obs}(H \to F)}{\sigma_H^{th}\ Br^{th}(H \to F)} \ , \tag{4.1}$$

where σ_H^{th} and $Br^{th}(H \to F)$ are the Standard Model predictions for the inclusive production cross section and the relevant branching ratio assuming that the H resonance is the Higgs boson. It is useful to introduce the following interaction strength for the η_{gt} meson:

$$\mu_F^{\eta_{gt}} \ = \ \frac{\sigma_{\eta_{gt}}^{th}\ Br^{th}(\eta_{gt} \to F)}{\sigma_H^{th}\ Br^{th}(H \to F)} \ . \tag{4.2}$$

In fact, if the LHC H resonance turns out to be the η_{gt} meson, then the measured interaction strengths should satisfy:

$$\mu_F \ \simeq \ \mu_F^{\eta_{gt}} \ . \tag{4.3}$$

We see, then, that to compare quantitatively our theoretical proposal with observations it is enough to estimate the interaction strengths $\mu_F^{\eta_{gt}}$, Eq. (4.2). In Sect. 3.5 we already estimated the η_{gt} meson branching ratios. Therefore, now it is necessary to evaluate the η_{gt} inclusive production cross section. Since the η_{gt} meson is an admixture of the pseudoscalar glueball η_g and the pseudoscalar $t\bar{t}$ bound state η_t, the production cross section can be estimated from the production cross sections of the relevant hadronic bound states. Unfortunately, the production mechanisms of a given bound state in hadron collisions at high energies is strongly model dependent. Moreover, no single hadro-production model is able to describe all the experimental data (see, eg, Ref. [47] and references therein). Actually, in several models to describe heavy quarkonium $q\bar{q}$ bound-state production the inclusive cross section is expected to be a fraction $\mathcal{F}$ of the cross section of the produced $q\bar{q}$ pairs. Indeed, these model are still widely used as simulation benchmark since, once the fractions are determined, it has a full predicting power about cross sections. In this

$\sqrt{s}\,(TeV)$	$\sigma^{th}_{t\bar{t}}(pb)$	$\sigma^{th}_{\eta_{gt}}(pb)$	$\sigma^{th}_{H}(pb)$	$\sigma^{obs}_{H}(pb)$
7	$173.60^{+11.25}_{-11.79}$	$15.20^{+0.98}_{-1.03}$	17.4 ± 1.6	$22.1^{+7.5}_{-5.9}$
8	$247.74^{+16.02}_{-15.94}$	$21.69^{+1.40}_{-1.40}$	22.3 ± 2.0	$27.7^{+3.8}_{-3.6}$
13	$815.96^{+45.51}_{-49.82}$	$71.44^{+3.98}_{-4.36}$	$55.5^{+2.4}_{-3.4}$	$59.0^{+10.7}_{-9.8}$

Table 2: Summary of the production inclusive cross sections at $\sqrt{s} = 7, 8, 13\,TeV$.

case, the coupling of a specific bound state to the $q\bar{q}$ pair is directly determined by the appropriate wave function which includes all relevant quantum number projections in conformity with the spin, angular momentum, charge conjugation and the color singlet nature of the bound state considered. We already observed that, since $m_t \gg m_{\eta_g}$, the $t\bar{t}$ bound-state wave function overwhelms the pseudoscalar glueball wave function. Therefore, naively, one expects that the main production mechanism of the η_{gt} meson is through $t\bar{t}$ pairs. However, one should keep in mind that the production cross section of two gluons is expected to exceed the $t\bar{t}$ cross section by orders of magnitude. So that, in general, both mechanisms should contribute to the associated production of the η_{gt} pseudoscalar meson. Nevertheless, we shall assume that the main production mechanism is due to the inclusive $t\bar{t}$ cross section. This is certainly a rather crude procedure, yet the resulting values for the inclusive production cross sections should be reliable enough to our purposes. According to our previous discussion, we assume that:

$$\sigma^{th}_{\eta_{gt}} \;\simeq\; \mathcal{F}\,\sigma^{th}_{t\bar{t}} \;\; . \tag{4.4}$$

For the theoretical $t\bar{t}$ pair production cross section we use the top-quark-pair cross section available in Ref. [48].
In Table 2 we report the inclusive $t\bar{t}$ cross sections at $\sqrt{s} = 7, 8, 13\,TeV$. To determine the parameter $\mathcal{F}$ we impose that at $\sqrt{s} = 8\,TeV$:

$$\sigma^{th}_{\eta_{gt}}(\sqrt{s} = 8\,TeV) \;\simeq\; \sigma^{th}_{H}(\sqrt{s} = 8\,TeV) \;\; , \tag{4.5}$$

where σ^{th}_{H} is the theoretical inclusive production cross section of the Standard Model Higgs boson, also displayed in Table 2. At $\sqrt{s} = 7, 8\,TeV$ the theoretical inclusive Higgs boson production cross sections have been taken from Table 1 in Ref. [10], while at $\sqrt{s} = 13\,TeV$ the theoretical Higgs production cross section has been taken from Table 8 in Ref. [49]. From Table 2 and Eq. (4.5) we readily obtain:

$$\mathcal{F} \;\simeq\; 0.0876 \;\; . \tag{4.6}$$

After that, our estimate for the inclusive production cross section of the η_{gt} pseudoscalar resonance is based on Eqs. (4.4) and (4.6). For comparison, in Table 2 we report the observed production cross section of the H resonance. At $\sqrt{s} = 7, 8\,TeV$ the observed production cross section of the H resonance is taken from Table 5 in Ref. [10]. At $\sqrt{s} = 13\,TeV$ the observed H boson production cross section is based on the combined measurements using more than $13.3\,fb^{-1}$ of proton-proton collision data recorded by the ATLAS experiment at the LHC at $\sqrt{s} = 13\,TeV$. The combination is based on the analyses of the H resonance decays into $\gamma\gamma$ and $ZZ \to 4\ell$ [49]. Remarkably, we see that the

our estimate of the η_{gt} production cross sections are comparable to the theoretical Higgs production cross sections. Moreover, both cross sections are in reasonable agreement with the experimental H boson production cross sections.

Having determined the inclusive production cross sections of the pseudoscalar meson

Decay Channel	ATLAS	CMS	η_{gt}
μ_{ZZ}	$1.52^{+0.40}_{-0.34}$	$1.04^{+0.32}_{-0.26}$	1.05 ± 0.10
μ_{WW}	$1.22^{+0.25}_{-0.21}$	$0.90^{+0.25}_{-0.21}$	1.03 ± 0.11
$\mu_{\gamma\gamma}$	$1.14^{+0.27}_{-0.25}$	$1.11^{+0.25}_{-0.23}$	0.94 ± 0.10
$\mu_{Z\gamma}$	$2.7^{+4.5}_{-4.3}$	$2.7^{+4.5}_{-4.3}$	2.18 ± 0.24
$\mu_{b\bar{b}}$	$0.62^{+0.37}_{-0.37}$	$0.81^{+0.45}_{-0.43}$	0.00052 ± 0.00006
$\mu_{\tau^+\tau^-}$	$1.41^{+0.40}_{-0.38}$	$0.88^{+0.30}_{-0.28}$	0.00020 ± 0.00002

Table 3: The measurements of the H resonance interaction strengths performed by ATLAS and CMS experiments on data collected during the LHC Run 1. The data have been taken from Table 5 in Ref. [11]. Estimates of the interaction strengths for the η_{gt} resonance as given by Eq. (4.2).

η_{gt}, we may evaluate the interaction strengths Eq. (4.2). Our results are displayed in Table 3 together with the measurements of the H resonance interaction strengths performed by ATLAS and CMS experiments on data collected during the LHC Run 1. We see that, within the statistical uncertainties, the η_{gt} interaction strengths are in fair good agreements with observations in the vector boson decay channels. On the other hand, for the decays into fermions , the η_{gt} interaction strengths are vanishingly small. Therefore, we are suggesting that to identify the new LHC resonance with the Standard Model Higgs boson it is of fundamental importance to determine experimentally the coupling to fermions to a high degree of statistical significance. Fortunately, the Run 2 of the LHC at $\sqrt{s} = 13\,TeV$ is now making an even larger sample of H boson events available for analysis. Nevertheless, the preliminary data from Run 2 does not show yet statistically convincing evidences of the decay $H \to b\bar{b}$, that should be the dominant decay mode of the Standard Model Higgs boson. On the other hand, we already noticed that the both ATLAS and CMS experiments reported new measurements of the $\mu_{t\bar{t}H}$ interaction strength confirming an enhanced coupling of the H boson to the top quarks. Note that, within our approach this enhancement with respect to theoretical expectations simply means that the production cross section of the η_{gt} meson associated to a $t\bar{t}$ pair is about a factor two higher with respect to the Standard Model Higgs boson. In any case, we feel that will be interesting to follow as more data are recorded.

5 The H_T Higgs Boson

In Ref. [1] it was discussed the scenario where the Higgs boson without self-interaction could coexist with the spontaneous symmetry breaking of the gauge symmetries. In that case, as we said in Sect. 1, the relation between Higgs mass and the physical Higgs condensate is not the same as in perturbation theory leading to the remarkable prediction Eq. (1.4) that implies a rather massive Higgs boson, $m_{H_T} \simeq 750\,GeV$. The coupling of the

Higgs field to the gauge vector bosons is fixed by the gauge symmetries. Therefore, the coupling of the H_T Higgs boson to the gauge vector bosons is the same as in perturbation theory notwithstanding the non perturbative Higgs condensation driving the spontaneous breaking of the gauge symmetries. Given the rather large mass of the H_T Higgs boson, the main decay modes are the decays into two massive vector bosons (see, e.g., Refs. [50, 51]):

$$\Gamma(H_T \,\to\, W^+\,W^-) \,\simeq\, \frac{G_F\,m_{H_T}^3}{8\pi\sqrt{2}}\,\sqrt{1-\frac{4m_W^2}{m_{H_T}^2}}\,\left(1-4\,\frac{m_W^2}{m_{H_T}^2}+12\,\frac{m_W^4}{m_{H_T}^4}\right) \tag{5.1}$$

and

$$\Gamma(H_T \,\to\, Z^0\,Z^0) \,\simeq\, \frac{G_F\,m_{H_T}^3}{16\pi\sqrt{2}}\,\sqrt{1-\frac{4m_Z^2}{m_{H_T}^2}}\,\left(1-4\,\frac{m_Z^2}{m_{H_T}^2}+12\,\frac{m_Z^4}{m_{H_T}^4}\right)\,. \tag{5.2}$$

On the other hand, it is known that for heavy Higgs the radiative corrections to the decay widths can be safely neglected [52, 53, 54].
The couplings of the H_T Higgs boson to the fermions are given by the Yukawa couplings λ_f. Unfortunately, there are not reliable lattice non-perturbative simulations on the continuum limit of the Yukawa couplings. If we follow the perturbative approximation, then the fermion Yukawa couplings turn out to be proportional to the fermion mass, $\lambda_f = m_f/v$. In that case, for heavy Higgs the only relevant fermion coupling is the top Yukawa coupling λ_t. On the other hand, we cannot exclude that the couplings of the physical Higgs field to the fermions could be very different from perturbation theory. Therefore, to parametrize our ignorance on the Yukawa couplings of the H_T Higgs boson we introduce the parameter:

$$\kappa \;=\; \lambda_t^2\,\frac{v^2}{m_t^2}\,. \tag{5.3}$$

Obviously, in perturbation theory we have $\kappa = 1$. However, we shall also consider the case of $\kappa \simeq 0$ corresponding to strongly suppressed fermion Yukawa couplings.
The width for the decays of the H_T boson into a $t\bar{t}$ pairs is easily found [50, 51]:

$$\Gamma(H_T \to\, t\,\bar{t}) \,\simeq\, \kappa\,\frac{3\,G_F\,m_{H_T}m_t^2}{4\pi\,\sqrt{2}}\,\left(1-4\,\frac{m_t^2}{m_{H_T}^2}\right)^{\frac{3}{2}}\,. \tag{5.4}$$

So that, to a good approximation, the Higgs total width is given by:

$$\Gamma_{H_T} \,\simeq\, \Gamma(H_T \to W^+\,W^-) \,+\, \Gamma(H_T \to Z^0\,Z^0) \,+\, \Gamma(H_T \to t\,\bar{t})\,. \tag{5.5}$$

In Fig. 4, left panel, we display the total width Γ_{H_T}, Eq. (5.5), versus the H_T Higgs mass for both $\kappa = 1$ and $\kappa = 0$. We see that, in the high mass region $m_{H_T} \gtrsim 400\,GeV$ the total width depends strongly on the Higgs mass. The main difficulty in the experimental identification of a very heavy Higgs resides in the large width which makes almost impossible to observe a mass peak. In fact, the expected mass spectrum of our heavy Higgs should be proportional to the Lorentzian distribution. Indeed, for a resonance with mass M and total width Γ the Lorentzian distribution is given by:

$$L(E) \;\sim\; \frac{\Gamma}{(E\,-\,M^2)^2\,+\,\Gamma^2/4}\,. \tag{5.6}$$

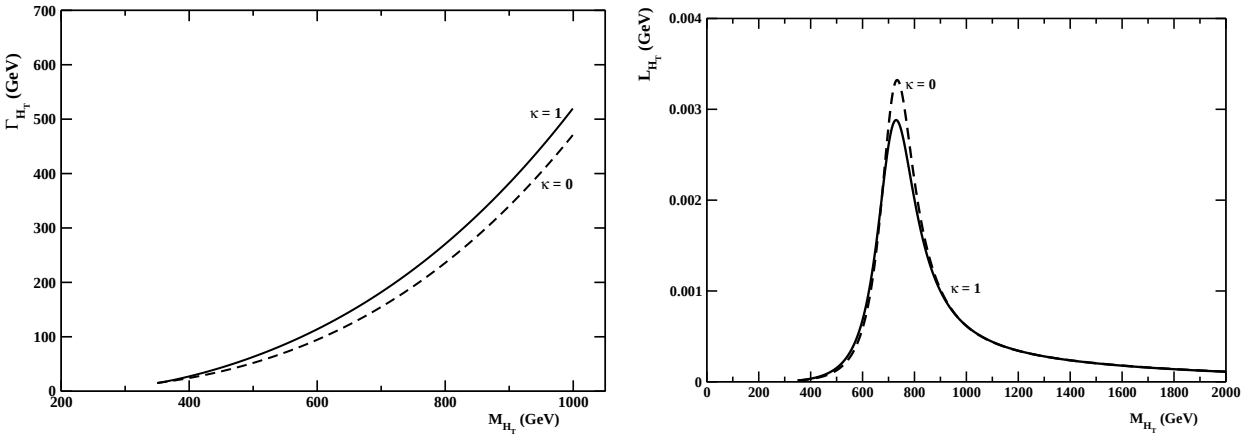

Figure 4: The H_T Higgs total width (left panel) and Lorentzian distribution (right panel) versus m_{H_T} for $\kappa = 1$ (full line) and $\kappa = 0$ (dashed line).

Note that Eq. (5.6) is the simplest distribution consistent with the Heisenberg uncertainty principle and the finite lifetime $\tau \simeq 1/\Gamma$. We obtain, therefore, the following Lorentzian distribution (see Fig. 4, right panel):

$$L_{H_T}(E) \;\simeq\; \frac{1}{1.0325\,\pi}\,\frac{\frac{\Gamma_{H_T}(E)}{2}}{\left(E\;-\;750\,GeV\right)^2\;+\;\left(\frac{\Gamma_{H_T}(E)}{2}\right)^2}\quad , \tag{5.7}$$

where $\Gamma_{H_T}(E)$ is given by Eq. (5.5), and the normalization is such that:

$$\int_0^\infty\; L_{H_T}(E)\,dE\;\;=\;\;1\;\;. \tag{5.8}$$

Note that, in the limit $\Gamma_{H_T}\;\to\;0$, $L_{H_T}(E)$ reduces to $\delta(E\;-750\,GeV)$.
To evaluate the Higgs event production at LHC we need the inclusive Higgs production cross section. As in perturbation theory, for large Higgs masses the main production processes are by vector-boson fusion and gluon-gluon fusion. In fact, the H_T Higgs production cross section by vector-boson fusion is the same as in the perturbative Standard Model calculations. Moreover, for Higgs mass in the range $700 - 800\,GeV$ the main production mechanism at LHC is expected to be by the gluon fusion mechanism. The gluon coupling to the Higgs boson in the Standard Model is mediated by triangular loops of top and bottom quarks. Since in perturbation theory the Yukawa couplings of the Higgs particle to heavy quarks grows with quark mass, thus balancing the decrease of the triangle amplitude, the effective gluon coupling approaches a non-zero value for large loop-quark masses. This means that for heavy Higgs the gluon fusion inclusive cross section is almost completely determined by the top quarks, even though it is interesting to stress that for large Higgs masses the vector-boson fusion mechanism becomes competitive to the gluon fusion Higgs production. According to our approximations the total inclusive cross section for the production of the H_T Higgs boson can be written as:

$$\sigma(p\,p\;\to\;H_T\;+\;X)\;\simeq\;\sigma_{VV}(p\,p\;\to\;H_T\;+\;X)\;+\;\kappa\,\sigma_{gg}(p\,p\;\to\;H_T\;+\;X)\,, \tag{5.9}$$

where σ_{VV} and σ_{gg} are the vector-boson fusion and gluon-gluon fusion inclusive cross sections respectively.

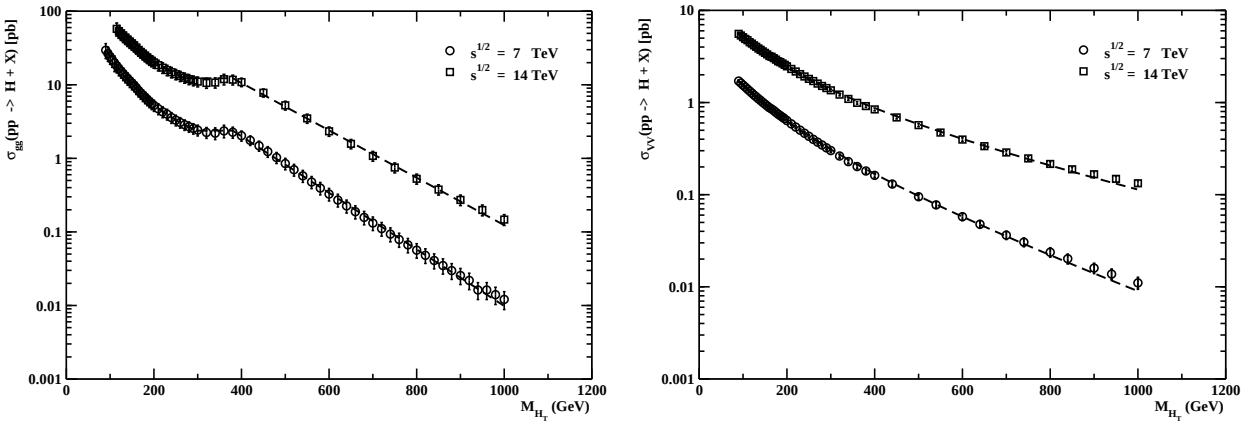

Figure 5: The inclusive Higgs production gluon-gluon fusion (left) and vector-boson fusion cross sections (right). Open circles and squares correspond to the cross sections at $\sqrt{s} = 7, 14\, TeV$ respectively. The data have been taken from Ref. [55]. The dashed lines are the fits of the data to our parametrization Eqs. (5.10) and (5.12).

In Ref. [55] it is presented the calculations of the cross sections computed at next-to-next-to-leading and next-to-leading order for each of the production modes at $\sqrt{s} = 7, 8, 14\, TeV$. In Fig. 5 we show the dependence on the Higgs mass of the perturbative gluon-gluon (left panel) and vector-boson fusion (right panel) cross sections at $\sqrt{s} = 7, 14\, TeV$ as reported in Ref. [55]. As concern the gluon-gluon fusion cross section at $\sqrt{s} = 14\, TeV$ we found that this cross section can be parametrized as:

$$\sigma_{gg}(p\,p \;\rightarrow\; H_T + X) \;\simeq\; \begin{cases} \left(\frac{a_1}{M_{H_T}} \;+\; a_2\; M_{H_T}^3\right)\; \exp(-a_3 M_{H_T}) & M_{H_T} \;\leq\; 273\; GeV \\ a_4 & 273\; GeV \leq M_{H_T} \leq 380\; GeV \\ a_4\; \exp\left[\,-a_5 (M_{H_T} - 380\; GeV)\right] & 380\; GeV \;\leq\; M_{H_T} \end{cases} \tag{5.10}$$

where M_{H_T} is expressed in GeV. In fact we fitted Eq. (5.10) to the data (see the dashed line in Fig. 5, left panel) and obtained:

$$\begin{aligned} &a_1 \simeq 3.55\, 10^4\; pb\, GeV \;\;,\;\; a_2 \simeq 3.16\, 10^{-5}\; pb\, GeV^{-3}\;, \\ &a_3 \simeq 1.52\, 10^{-2}\; GeV^{-1}\;,\;\; a_4 \simeq 12.27\;\; pb\;, \\ &a_5 \simeq 7.42\, 10^{-3}\; GeV^{-1}\;. \end{aligned} \tag{5.11}$$

Likewise, we parametrized the dependence of the vector-boson fusion cross section as:

$$\sigma_{VV}(p\,p \;\rightarrow\; H_T \;+\; X) \;\simeq\; \left(b_1 \;+\; \frac{b_2}{M_{H_T}} \;+\; \frac{b_3}{M_{H_T}^2}\right)\; \exp(-b_4\; M_{H_T})\;, \tag{5.12}$$

and obtained for the best fit (see the dashed line in Fig. 5, right panel) :

$$\begin{aligned} &b_1 \simeq 3.08\, 10^{-6}\; pb \;\;,\;\; b_2 \simeq 7.95\, 10^2\; pb\, GeV\;, \\ &b_3 \simeq -1.64\, 10^4\; pb\, GeV^2 \;\;,\; b_4 \simeq 1.92\, 10^{-3}\; GeV^{-1}\;. \end{aligned} \tag{5.13}$$

We have explicitly checked that the same parameterizations are valid also at $\sqrt{s} = 7, 8\, TeV$ (see Fig. 5).

5.1 H_T Decay Channels

We have seen that the main decays of the heavy H_T Higgs boson are the decays into two massive vector boson and $t\bar{t}$ pairs, if $\kappa = 1$. Since the search for the decays of the H_T Higgs boson into pairs of top quarks is very complicated because of the large QCD background, we will focus on the decays into two massive vector bosons [5].
To compare the invariant mass spectrum of our H_T Higgs with the experimental data, we observe that:

$$N_{H_T}(E_1, E_2) \simeq \mathcal{L} \int_{E_1}^{E_2} Br(E)\, \varepsilon(E)\, \sigma(p\, p \rightarrow H_T + X)\, L_{H_T}(E)\, dE \ , \qquad (5.14)$$

where N_{H_T} is the number of Higgs events in the energy interval E_1, E_2, corresponding to an integrated luminosity $\mathcal{L}$, in the given channel with branching ratio $Br(E)$. The parameter $\varepsilon(E)$ accounts for the efficiency of trigger, acceptance of the detectors, the kinematic selections, and so on. Thus, in general $\varepsilon(E)$ depends on the energy, the selected channel and the detector. For illustrative purposes, we consider the decay channels $H \rightarrow WW \rightarrow \ell\nu qq$ and $H \rightarrow ZZ \rightarrow \ell\ell qq$. As concern the branching ratios Br(E), we can write:

$$\begin{array}{l} Br(H_T \rightarrow WW \rightarrow \ell\nu qq) \simeq Br(H_T \rightarrow WW) \times Br(WW \rightarrow \ell\nu qq) \\ Br(H_T \rightarrow ZZ \rightarrow \ell\ell qq) \simeq Br(H_T \rightarrow ZZ) \times Br(ZZ \rightarrow \ell\ell qq) \ , \end{array} \qquad (5.15)$$

where

$$Br(H_T \rightarrow WW) = \frac{\Gamma(H_T \rightarrow WW)}{\Gamma_{H_T}} \ , \ Br(H_T \rightarrow ZZ) = \frac{\Gamma(H_T \rightarrow ZZ)}{\Gamma_{H_T}} \ , \qquad (5.16)$$

and the branching ratios for the decays of W and Z bosons into fermions are given by the Standard Model values [58].
In Fig. 6 we display the distribution of the invariant mass for the Higgs boson candidates corresponding to the process $H_T \rightarrow WW \rightarrow \ell\nu qq$ (left) and the distribution of the invariant mass for the process $H_T \rightarrow ZZ \rightarrow \ell\ell qq$ (right). The distributions have been obtained using Eq. (5.14) with an integrated luminosity $\mathcal{L} = 30\, fb^{-1}$ for both $\kappa = 1$ and $\kappa = 0$. We used the Higgs inclusive cross section at $\sqrt{s} = 14\, TeV$ scaled by about 10% as our estimate of the cross section at $\sqrt{s} = 13\, TeV$. From Fig. 6 we see that the search strategy is to find some structures in the invariant mass spectrum. However, one should keep in mind that such strategy is severely hampered by the presence of the so-called irreducible background. The main backgrounds are given by the production of $W + jet$ and $Z + jet$ which, however, should be suppressed for large invariant mass. Moreover, the presence of charged lepton should allows to obtain a good rejection of the QCD processes.

It is interesting to mention that preliminary results from the ATLAS collaboration reported the experimental search of large mass resonances in the decay to WW final states, with one W boson decaying into an electron or a muon and a neutrino while the other W boson decaying hadronically [59]. The data correspond to an integrated luminosity of $13.2\, fb^{-1}$ collected by the ATLAS detector at $\sqrt{s} = 13\, TeV$. The data hint to an excess in the invariant mass distribution around $700\, GeV$ that, however, is not yet

[5] It is worthwhile to stress that the H_T decay to $\gamma\gamma$ do not proceed directly, but, to a fair good approximation, via longitudinal W virtual states. Therefore the relevant branching ratio turns out be strongly suppressed, i.e. $Br(H_T \rightarrow \gamma\gamma) \sim 10^{-6}$ [56, 57].

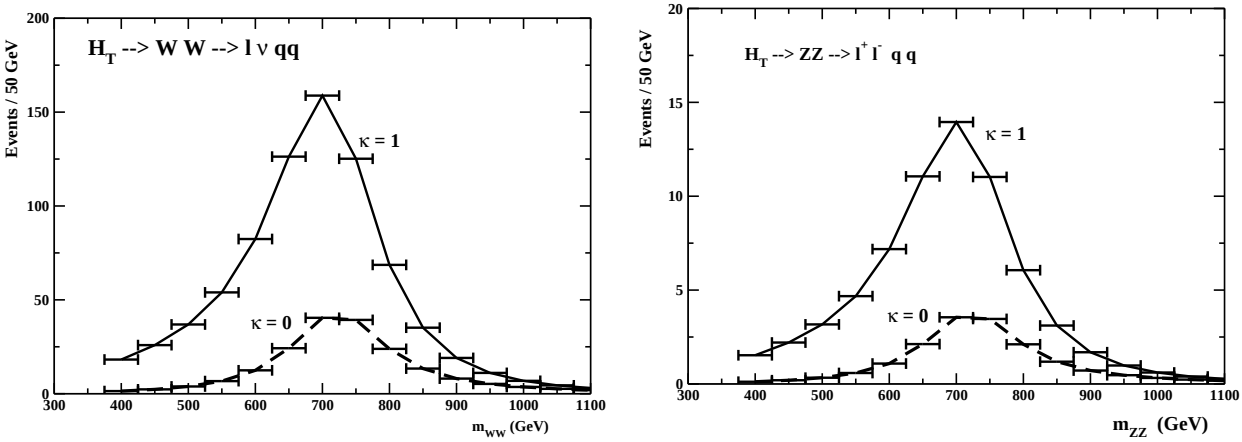

Figure 6: (Left) Distribution of the invariant mass m_{WW} for the process $H_T \to WW \to \ell\nu qq$ ($\ell = e, \mu$) corresponding to an integrated luminosity of 30 fb^{-1}. The H_T Higgs event distribution (binned in energy intervals of $50\,GeV$) are evaluated according to Eq. (5.14) assuming $\varepsilon(E) \simeq 0.20$, $\kappa = 1$ and $\kappa = 0$. (Right) Distribution of the invariant mass m_{ZZ} for the process $H_T \to ZZ \to \ell\ell qq$ ($\ell = e, \mu$) corresponding to an integrated luminosity of $30 fb^{-1}$.

statistical significant. Likewise, in Ref. [60] it is reported the searches for heavy resonance decaying into ZZ pair using collision data at $\sqrt{s} = 13\,TeV$ at the Large Hadron Collider corresponding to an integrated luminosity of $13.2\,fb^{-1}$ recorded with the ATLAS detector in 2015 and 2016. In the final states in which one Z boson decays to a pair of light charged leptons (electrons or muons) and the other Z boson decays into hadrons there is some excess in the invariant mass distribution near $700\,GeV$ for the vector-boson fusion production processes. However, it should be mentioned that the eventual signal is not statistically significant due to the low integrated luminosity.

5.2 The Golden Channel: Comparison with the LHC Data

The decay channels $H_T \to ZZ \to \ell\ell\ell\ell$ (the golden channel) have very low branching ratios. Nevertheless, the presence of leptons allows to efficiently reduce the huge background due mainly to diboson production. In this Section we attempt a quantitative comparison of our theoretical expectations with the experimental data from LHC Run 2. To increase the integrated luminosity we decided to combine the experimental data from both ATLAS [61] and CMS [62] experiments. In Fig. 7 we show the invariant mass distribution for the golden channel obtained by combining the data from the ATLAS experiment with an integrated luminosity of $14.8\,fb^{-1}$ [61] and the CMS experiment with an integrated luminosity of $12.9\,fb^{-1}$ [62]. From our estimate of the background (dotted line in Fig. 7) we see that, indeed, in the high invariant mass region $m_{ZZ} \gtrsim 600\,GeV$, the background is strongly suppressed. To compare with our theoretical expectations, we displayed in Fig. 7 the invariant mass distribution corresponding to the signal plus the background (full line). Due to the rather low integrated luminosity, we see that the signal manifest itself as an approximate plateaux in the invariant mass interval $600\,GeV \lesssim m_{ZZ} \lesssim 740\,GeV$ over a smoothly decreasing background. Actually, in this region it seems that there is a moderate excess of signal over the expected background that seems to compare quite well with our

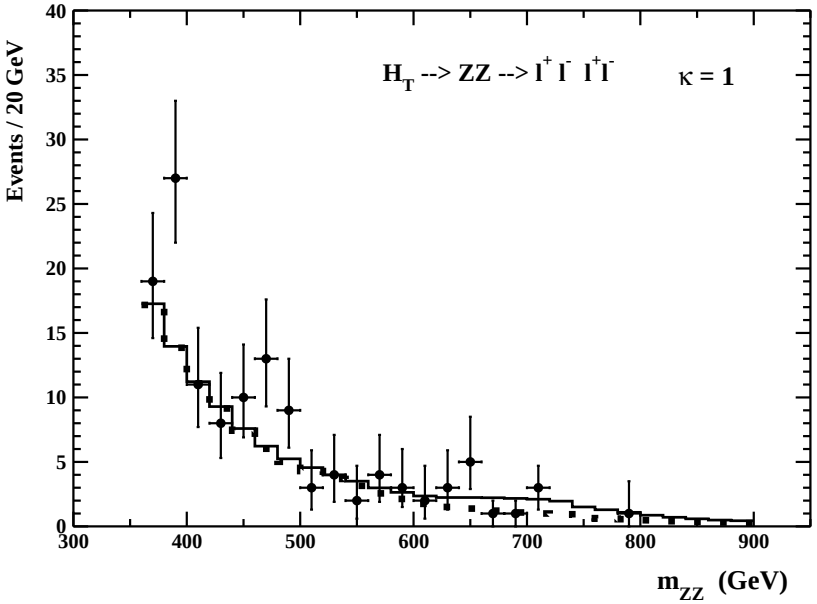

Figure 7: Comparison to the LHC data of the distribution of the invariant mass m_{ZZ} for the process $H_T \to ZZ \to \ell\ell\ell\ell$ ($\ell = e, \mu$) corresponding to an integrated luminosity of $\mathcal{L} \simeq 27.7\, fb^{-1}$ binned in energy intervals of $20\, GeV$ and assuming $\kappa = 1$. The data have been obtained combining the Run 2 LHC data at $\sqrt{s} = 13\, TeV$ from ATLAS [61] and CMS [62] with integrated luminosity $\mathcal{L} = 14.8\, fb^{-1}$ and $12.9\, fb^{-1}$ respectively. The dotted line is our estimate of the background, the continuum line is the background plus signal histogram assuming $\varepsilon(E) \simeq 0.48$ and $\kappa = 1$.

theoretical prediction. To be qualitative, we estimated the total number of events in the invariant mass interval $600\, GeV \lesssim m_{ZZ} \lesssim 740\, GeV$. We found that the expected background event was $N_{back} = 8.8$, while our theoretical estimate of the signal was $N^{th}_{sign} = 6.5$. The observed events in the given interval was $N_{obs} = 15.0^{+5.5}_{-3.4}$ where, to be conservative, the quoted errors have been obtained by adding in quadrature the experimental errors. So that there is an excess over the expected background with a statistical significance of about $2\,\sigma$ that is in fair agreement with the theoretical expectations. Therefore, our H_T Higgs event distribution in the golden channel is not in contradiction with the experimental data, even though we cannot exclude that the data are compatible with the background-only hypothesis. In fact, we estimated that to meet to the $5\,\sigma$ criterion in High Energy Physics it will be necessary to collect an integrated luminosity $\mathcal{L} \sim 10^2\, fb^{-1}$.

6 Conclusion

It is widely believed that the new LHC resonance at $125\, GeV$, denoted by H, is the Standard Model Higgs boson. The main motivation for this identification resides in the observed decays of the H resonance into vector bosons that agree to a high level of statistical significance with the expected rates of the Standard Model Higgs boson. To firmly establish that the H resonance is, indeed, the Standard Model Higgs boson, it is necessary to demonstrate the direct coupling to fermions. If the H resonance is identified with

the Higgs boson, then the largest branching ratio should be in the decays into bottom-antibottom pair. However, the data collected in the LHC Run 1 by both ATLAS and CMS experiments display a puzzling deficit in this channel. Moreover, the preliminary data at $\sqrt{s} = 13\,TeV$ still do not show a clear evidence for the decays in $b\bar{b}$ pair. On the other hand, we already pointed out that from LHC Run 1 and Run 2 data one infers an enhancement of the H resonance coupling to the top quark. The forthcoming data from the LHC Run 2 experiments will be of fundamental importance to settle these problems. In the meantime we believe that there are already compelling reasons to look for different explanations of the H resonance. In the first part of the present paper, following Ref. [20], we advanced the proposal that the H resonance could be a pseudoscalar meson. We developed a phenomenological approach where the H boson is a coherent superimposition of the low-lying pseudoscalar glueball and the $t\bar{t}$ bound state. We showed that this peculiar pseudoscalar meson is able to mimic the decays in vector bosons at the same rate as the Standard Model Higgs boson with the same mass. We pointed out that, once the decays into two vector bosons cannot be used to identity univocally the Higgs boson, to unravel the true nature of the H resonance it is necessary to rely on the decays into fermions and on the resonance CP assignment where, however, the reached statistical significance is still below the High Energy criterion of $5\,\sigma$. Finally, we would like to point out that in this paper we attempted an alternative interpretation of the new LHC resonance entirely within the Standard Model. However, at present we cannot exclude different possibilities beyond the Standard Model Physics.

In the second part of the present paper we focussed on the true Higgs boson denoted by H_T. Stemming from the known triviality problem, i.e. vanishing self-coupling, that affects self-interacting scalar quantum fields in four space-time dimensions, we evidenced that the Higgs boson condensation triggering the spontaneous breaking of the local gauge symmetries needs to be dealt with non perturbatively. In this case, from one hand there is no stability problem for the condensate ground state, on the other hand the Higgs mass is finitely related to the vacuum expectation value of the quantum scalar field and, in principle, it can be evaluated from first principles. In fact, precise non-perturbative numerical simulations indicated that the H_T Higgs boson mass is consistent with Eq. (1.4) [1] leading to a rather heavy Higgs boson. We critically discussed the couplings of the H_T Higgs boson to the massive vector bosons and to fermions. We estimated the expected production mechanism and the main decay modes. Finally, we, also, compared our proposal with the recent results in the golden channel from ATLAS and CMS collaborations. We found that the available experimental observations are not in contradiction with our scenario. We are confident that forthcoming data from LHC Run 2 will add further support to the heavy Higgs proposal.

References

[1] P. Cea and L. Cosmai, *The Higgs boson: From the lattice to LHC*, ISRN High Energy Physics, vol. 2012, Article ID 637950, arXiv:0911.5220.

[2] F. Englert and R. Brout, Phys. Rev. Lett. **13** (1964) 321.

[3] P. Higgs, Phys. Lett. **12** (1964) 132.

[4] G. Guralnik, C. Hagen and T. Kibble, Phys. Rev. Lett. **13** (1964) 585.

[5] P. Higgs, Phys. Rev. **145** (1966) 1156.

[6] The ATLAS Collaboration, G. Aad, *et al.*, Phys. Lett. B **716** (2012) 1.

[7] The CMS Collaboration, S. Chatrchyan, *et al.*, Phys. Lett. B **716** (2012) 30.

[8] The ATLAS and CMS Collaborations, Phys. Rev. Lett. **114** (2015) 191803.

[9] The CMS Collaboration, Eur. Phys. J. C **75** (2015) 212.

[10] The ATLAS Collaboration, Eur. Phys. J. C **76** (2016) 6.

[11] The ATLAS and CMS Collaborations, JHEP **08** (2016) 045.

[12] The ATLAS Collaboration, JHEP **01** (2015) 069.

[13] The CMS Collaboration, Phys. Rev. D **89** (2014) 012003.

[14] The ATLAS Collaboration, JHEP **04** (2015) 117.

[15] The CMS Collaboration, JHEP **05** (2014) 104.

[16] The ATLAS Collaboration, Eur. Phys. J. C **75** (2015) 476.

[17] The CMS Collaboration, Phys. Rev. D **92** (2015) 012004.

[18] The ATLAS Collaborations, *Combination of the searches for Higgs boson production in association with top quarks in the $\gamma\gamma$, multilepton, and $b\bar{b}$ decay channels at $\sqrt{s} = 13\,TeV$ with the ATLAS Detector*, ATLAS-CONF-2016-068 (2016).

[19] The CMS Collaborations, *Search for associated production of Higgs bosons and top quarks in multilepton final states at $\sqrt{s} = 13\,TeV$*, CMS PAS HIG-16-022 (2016).

[20] P. Cea, *Comment on the evidence of the Higgs boson at LHC*, arXiv:1209.3106 [hep-ph].

[21] R. Fernandez, J. Fröhlich, and A. D. Sokal, *RandomWalks, Critical Phenomena, and Triviality in Quantum Field Theory*, Springer, Berlin, Germany, 1992.

[22] The ATLAS Collaboration, M. Aaboud, *et al.* , JHEP **09** (2016) 001.

[23] The CMS Collaboration, V. Khachatryan, *et al.*, Phys. Rev. Lett. **117** (2016) 051802.

[24] The CMS Collaboration, *Search for resonant production of high mass photon pairs using $12.9\,fb^{-1}$ of proton-proton collisions at $\sqrt{s} = 13\,TeV$ and combined interpretation of searches at 8 and $13\,TeV$*, CMS PAS EXO-16-027 (2016).

[25] B. Lenzi, on behalf of the ATLAS Collaboration, *Search for a high mass diphoton resonance using the ATLAS detector*, *38th International Conference on High Energy Physics*, August 3 - 10 2016, Chicago.

[26] L. Carminati , *Diphoton Searches at ATLAS*, *Charting the Unknown: interpreting LHC data from the energy frontier* CERN TH Institute Workshop, 25 July - 12 August 2016, CERN.

[27] J. Bendavid, *Diphoton Searches at CMS*, *Charting the Unknown: interpreting LHC data from the energy frontier* CERN TH Institute Workshop, 25 July - 12 August 2016, CERN.

[28] E. Eichten, K. Gottfried, T. Kinoshita, K. D. Lane, and T. M. Yan, Phys. Rev. D **21** (1980) 203.

[29] J. L. Richardson, Phys. Lett. B **82** (1979) 272.

[30] P. Cea, and G. Nardulli, Phys. Rev. D **34** (1986) 1863.

[31] E. Klempt and A. Zaitsev, Phys. Rept. **454** (2007) 1.

[32] V. Crede and C. A. Meyer, Prog. Part. Nucl. Phys. **63** (2009) 74.

[33] T. Appelquist and H. D. Politzer, Phys. Rev. D **12** (1975) 1404.

[34] A. De Rújula, H. Georgi, and S. L. Glashow, Phys. Rev. D **12** (1975) 147.

[35] V. A. Novikov, *et al.*, Phys. Rep. C **41** (1978) 1

[36] F. E. Close, *An Introduction to Quarks and Partons*, Academic Press, London, New York, San Francisco (1979).

[37] T.-P. Chang and L.-F. Li, *Gauge Theory of Elementary Particle Physics*, Clarendon Press, Oxford (1982).

[38] J. H. Kühn, J. Kaplan, and G. Safiani, Nucl. Phys. B **157** (1979) 125.

[39] B. Guberina, J. H. Kühn, R. Peccei, and R. Rückl, Nucl. Phys. B **174** (1980) 317.

[40] J. H. Kühn, Acta Phys. Pol. B **12** (1981) 347.

[41] V. Barger, *et al.*, Phys. Rev. D **35** (1987) 3366.

[42] S. B. Treiman, R. Jackiw, B. Zumino, and E. Witten, *Current Algebra and Anomalies*, Princeton Series in Physics, World Scientific Publishing Co Pte Ltd. (1985).

[43] R. A. Bertlmann, *Anomalies in Quantum Field Theory*, Clarendon Press, Oxford (1996).

[44] M. S. Chanowitz, *Resonances in Photon-Photon Scattering*, talk given at the VI International Workshop on Photon-Photon Collisions (1984) LBL-18701.

[45] M. D. Scadron, Rep. Prog. Phys. **44** (1981) 213.

[46] *Handbook of of LHC Higgs Cross Sections: 3. Higgs Properties*, Editors: S. Heinemeyer, C. Mariotti, G. Passarino, and R. Tanaka, arXiv:1307.1347 [hep-ph].

[47] N. Brambilla, *et al.*, Eur. Phys. J. C **71** (2011) 1534.

[48] https://twiki.cern.ch/twiki/bin/view/LHCPhysics/TtbarNNLO.

[49] The ATLAS Collaboration, *Combined measurements of the Higgs boson production and decay rates in $H \to ZZ^* \to 4\ell$ and $H \to \gamma\gamma$ final states using pp collision data at $\sqrt{s} = 13\,TeV$ in the ATLAS experiment*, ATLAS-CONF-2016-081 (2016).

[50] J. F. Gunion, H. E. Haber, G. Kane, and S. Dawson, *The Higgs Hunter's Guide*, Perseus Publishing, Cambridge, Massachusetts (1990).

[51] A. Djouadi, Phys. Rept. **457** (2008) 1.

[52] J. Fleischer and F. Jegerlehmer, Phys. Rev. D **23** (1981) 2001.

[53] J. Fleischer and F. Jegerlehmer, Nucl. Phys. B **216** (1983) 469.

[54] W. J. Marciano and S. D. Willenbrok, Phys. Rev. D **37** (1988) 2509.

[55] *Handbook of LHC Higgs Cross Sections: 1. Inclusive Observables*, Editors: S. Dittmaier, C. Mariotti, G. Passarino, and R. Tanaka, arXiv:1101.0593 [hep-ph].

[56] J. R. Ellis, M. K. Gaillard, and D. V. Nanopoulos, Nucl. Phys. B **106** (1976) 292 .

[57] M. A. Shifman, A. I. Vainshtein, M. B. Voloshin, and V. I. Zakharov, Sov. J. Nucl. Phys. **30** (1979) 711.

[58] K. A. Olive, *et al.* (Particle Data Group), Chin. Phys. C **38** (2014) 090001.

[59] The ATLAS Collaboration, *Search for diboson resonance production in the $\ell\nu qq$ final state using p p collisions at $\sqrt{s} = 13\,TeV$ with the ATLAS detector at the LHC*, ATLAS-CONF-2016-062 (2016).

[60] The ATLAS Collaboration, *Searches for heavy ZZ and ZW resonances in the $\ell\ell qq$ and $\nu\nu qq$ final states in pp collisions at $\sqrt{s} = 13\,TeV$ with the ATLAS detector*, ATLAS-CONF-2016-082 (2016).

[61] The ATLAS Collaboration, *Study of the Higgs boson properties and search for high-mass scalar resonances in the $H \to ZZ^* \to 4\ell$ decay channel at $\sqrt{s} = 13\,TeV$ with the ATLAS detector*, ATLAS-CONF-2016-079 (2016).

[62] The CMS Collaboration, *Measurements of properties of the Higgs boson and search for an additional resonance in the four-lepton final state at $\sqrt{s} = 13\,TeV$*, CMS PAS HIG-16-033 (2016).